Proceedings

of the

XXVI Congreso de Ecuaciones Diferenciales y Aplicaciones
XVI Congreso de Matemática Aplicada

Gijón (Asturias), Spain

June 14-18, 2021

CEDYA CMA 2020 GIJÓN

SēMA
Sociedad Española de Matemática Aplicada

Universidad de Oviedo

Editors:
Rafael Gallego, Mariano Mateos

Universidad de Oviedo
Servicio de Publicaciones de la Universidad de Oviedo
Campus de Humanidades. Edificio de Servicios. 33011 Oviedo (Asturias)
Tel. 985 10 95 03 Fax 985 10 95 07
http: www.uniovi.es/publicaciones
servipub@uniovi.es

ISBN: 978-84-18482-21-2

Foreword

It is with great pleasure that we present the Proceedings of the 26th Congress of Differential Equations and Applications / 16th Congress of Applied Mathematics (XXVI CEDYA / XVI CMA), the biennial congress of the Spanish Society of Applied Mathematics S$\vec{e}$MA, which is held in Gijón, Spain from June 14 to June 18, 2021.

In this volume we gather the short papers sent by some of the almost three hundred and twenty communications presented in the conference. Abstracts of all those communications can be found in the abstract book of the congress. Moreover, full papers by invited lecturers will shortly appear in a special issue of the S$\vec{e}$MA Journal.

The first CEDYA was celebrated in 1978 in Madrid, and the first joint CEDYA / CMA took place in Málaga in 1989. Our congress focuses on different fields of applied mathematics: Dynamical Systems and Ordinary Differential Equations, Partial Differential Equations, Numerical Analysis and Simulation, Numerical Linear Algebra, Optimal Control and Inverse Problems and Applications of Mathematics to Industry, Social Sciences, and Biology. Communications in other related topics such as Scientific Computation, Approximation Theory, Discrete Mathematics and Mathematical Education are also common.

For the last few editions, the congress has been structured in mini-symposia. In Gijón, we will have eighteen minis-symposia, proposed by different researchers and groups, and also five thematic sessions organized by the local organizing committee to distribute the individual contributions. We will also have a poster session and ten invited lectures. Among all the mini-symposia, we want to highlight the one dedicated to the memory of our colleague Francisco Javier "Pancho" Sayas, which gathers two plenary lectures, thirty-six talks, and more than forty invited people that have expressed their wish to pay tribute to his figure and work.

This edition has been deeply marked by the COVID-19 pandemic. First scheduled for June 2020, we had to postpone it one year, and move to a hybrid format. Roughly half of the participants attended the conference online, while the other half came to Gijón. Taking a normal conference and moving to a hybrid format in one year has meant a lot of efforts from all the parties involved. Not only did we, as organizing committee, see how much of the work already done had to be undone and redone in a different way, but also the administration staff, the scientific committee, the mini-symposia organizers, and many of the contributors had to work overtime for the change.

Just to name a few of the problems that all of us faced: some of the already accepted mini-symposia and contributed talks had to be withdrawn for different reasons (mainly because of the lack of flexibility of the funding agencies); it became quite clear since the very first moment that, no matter how well things evolved, it would be nearly impossible for most international participants to come to Gijón; reservations with the hotels and contracts with the suppliers had to be cancelled; and there was a lot of uncertainty, and even anxiety could be said, until we were able to confirm that the face-to-face part of the congress could take place as planned.

On the other hand, in the new open call for scientific proposals, we had a nice surprise: many people that would have not been able to participate in the original congress were sending new ideas for mini-symposia, individual contributions and posters. This meant that the total number of communications was about twenty percent greater than the original one, with most of the new contributions sent by students.

There were almost one hundred and twenty students registered for this CEDYA / CMA. The hybrid format allows students to participate at very low expense for their funding agencies, and this gives them the opportunity to attend different conferences and get more merits. But this, which can be seen as an advantage, makes it harder for them to obtain a full conference experience. Alfréd Rényi said: "a mathematician is a device for turning coffee into theorems". Experience has taught us that a congress is the best place for a mathematician to have a lot of coffee. And coffee cannot be served online.

In Gijón, June 4, 2021

The Local Organizing Committee from the Universidad de Oviedo

Scientific Committee

- Juan Luis Vázquez, Universidad Autónoma de Madrid
- María Paz Calvo, Universidad de Valladolid
- Laura Grigori, INRIA Paris
- José Antonio Langa, Universidad de Sevilla
- Mikel Lezaun, Euskal Herriko Unibersitatea
- Peter Monk, University of Delaware
- Ira Neitzel, Universität Bonn
- JoséÁngel Rodríguez, Universidad de Oviedo
- Fernando de Terán, Universidad Carlos III de Madrid

Sponsors

- Sociedad Española de Matemática Aplicada
- Departamento de Matemáticas de la Universidad de Oviedo
- Escuela Politécnica de Ingeniería de Gijón
- Gijón Convention Bureau
- Ayuntamiento de Gijón

Local Organizing Committee from the Universidad de Oviedo

- Pedro Alonso Velázquez
- Rafael Gallego
- Mariano Mateos
- Omar Menéndez
- Virginia Selgas
- Marisa Serrano
- Jesús Suárez Pérez del Río

Contents

On numerical approximations to diffuse-interface tumor growth models
Acosta-Soba D., Guillén-González F. and Rodríguez-Galván J.R. **8**

An optimized sixth-order explicit RKN method to solve oscillating systems
Ahmed Demba M., Ramos H., Kumam P. and Watthayu W. **15**

The propagation of smallness property and its utility in controllability problems
Apraiz J. **23**

Theoretical and numerical results for some inverse problems for PDEs
Apraiz J., Doubova A., Fernández-Cara E. and Yamamoto M. **31**

Pricing TARN options with a stochastic local volatility model
Arregui I. and Ráfales J. **39**

XVA for American options with two stochastic factors: modelling, mathematical analysis and numerical methods
Arregui I., Salvador B., Ševčovič D. and Vázquez C. **44**

A numerical method to solve Maxwell's equations in 3D singular geometry
Assous F. and Raichik I. **51**

Analysis of a SEIRS metapopulation model with fast migration
Atienza P. and Sanz-Lorenzo L. **58**

Goal-oriented adaptive finite element methods with optimal computational complexity
Becker R., Gantner G., Innerberger M. and Praetorius D. **65**

On volume constraint problems related to the fractional Laplacian
Bellido J.C. and Ortega A. **73**

A semi-implicit Lagrange-projection-type finite volume scheme exactly well-balanced for 1D shallow-water system
Caballero-Cárdenas C., Castro M.J., Morales de Luna T. and Muñoz-Ruiz M.L. **82**

SEIRD model with nonlocal diffusion
Calvo Pereira A.N. **90**

Two-sided methods for the nonlinear eigenvalue problem
Campos C. and Roman J.E. **97**

Fractionary iterative methods for solving nonlinear problems
Candelario G., Cordero A., Torregrosa J.R. and Vassileva M.P. **105**

Well posedness and numerical solution of kinetic models for angiogenesis
Carpio A., Cebrián E. and Duro G. **109**

Variable time-step modal methods to integrate the time-dependent neutron diffusion equation
Carreño A., Vidal-Ferràndiz A., Ginestar D. and Verdú G. **114**

Homoclinic bifurcations in the unfolding of the nilpotent singularity of codimension 4 in R^4
Casas P.S., Drubi F. and Ibánez S. **122**

Different approximations of the parameter for low-order iterative methods with memory
Chicharro F.I., Garrido N., Sarría I. and Orcos L. **130**

Designing new derivative-free memory methods to solve nonlinear scalar problems
Cordero A., Garrido N., Torregrosa J.R. and Triguero P. **135**

Iterative processes with arbitrary order of convergence for approximating generalized inverses
Cordero A., Soto-Quirós P. and Torregrosa J.R. **141**

FCF formulation of Einstein equations: local uniqueness and numerical accuracy and stability
Cordero-Carrión I., Santos-Pérez S. and Cerdá-Durán P. **148**

New Galilean spacetimes to model an expanding universe
De la Fuente D. **155**

Numerical approximation of dispersive shallow flows on spherical coordinates
Escalante C. and Castro M.J. **160**

New contributions to the control of PDEs and their applications
Fernández-Cara E. **167**

Saddle-node bifurcation of canard limit cycles in piecewise linear systems
Fernández-García S., Carmona V. and Teruel A.E. **172**

On the amplitudes of spherical harmonics of gravitational potencial and generalised products of inertia
Floría L. **177**

Turing instability analysis of a singular cross-diffusion problem
Galiano G. and González-Tabernero V. **184**

Weakly nonlinear analysis of a system with nonlocal diffusion
Galiano G. and Velasco J. **192**

What is the humanitarian aid required after tsunami?
González-Vida J.M., Ortega S., Macías J., Castro M.J., Michelini A. and Azzarone A. **197**

On Keller-Segel systems with fractional diffusion
Granero-Belinchón R. **201**

An arbitrary high order ADER Discontinous Galerking (DG) numerical scheme for the multilayer shallow water model with variable density
Guerrero Fernández E., Castro Díaz M.J., Dumbser M. and Morales de Luna T. **208**

Picard-type iterations for solving Fredholm integral equations
Gutiérrez J.M. and Hernández-Verón M.A. **216**

High-order well-balanced methods for systems of balance laws based on collocation RK ODE solvers
Gómez-Bueno I., Castro M.J., Parés C. and Russo G. **220**

An algorithm to create conservative Galerkin projection between meshes
Gómez-Molina P., Sanz-Lorenzo L. and Carpio J. **228**

On iterative schemes for matrix equations
Hernández-Verón M.A. and Romero N. **236**

A predictor-corrector iterative scheme for improving the accessibility of the Steffensen-type methods
Hernández-Verón M.A., Magreñán A.A., Martínez E. and Sukhjit S. **242**

Recent developments in modeling free-surface flows with vertically-resolved velocity profiles using moments
Koellermeier J. **247**

Stability of a one degree of freedom Hamiltonian system in a case of zero quadratic and cubic terms
Lanchares V. and Bardin B. **253**

Minimal complexity of subharmonics in a class of planar periodic predator-prey models
López-Gómez J., Muñoz-Hernández E. and Zanolin F. **258**

On a non-linear system of PDEs with application to tumor identification
Maestre F. and Pedregal P. **265**

Fractional evolution equations in dicrete sequences spaces
Miana P.J. **271**

KPZ equation approximated by a nonlocal equation
Molino A. **277**

Symmetry analysis and conservation laws of a family of non-linear viscoelastic wave equations
Márquez A. and Bruzón M. **284**

Flux-corrected methods for chemotaxis equations
Navarro Izquierdo A.M., Redondo Neble M.V. and Rodríguez Galván J.R. **289**

Ejection-collision orbits in two degrees of freedom problems
Ollé M., Álvarez-Ramírez M., Barrabés E. and Medina M. **295**

Teaching experience in the Differential Equations Semi-Virtual Method course of the Tecnológico de Costa Rica
Oviedo N.G. **300**

Nonlinear analysis in lorentzian geometry: the maximal hypersurface equation in a generalized Robertson-Walker spacetime
Pelegrín J.A.S. **307**

Well-balanced algorithms for relativistic fluids on a Schwarzschild background
Pimentel-García E., Parés C. and LeFloch P.G. **313**

Asymptotic analysis of the behavior of a viscous fluid between two very close mobile surfaces
Rodríguez J.M. and Taboada-Vázquez R. **321**

Convergence rates for Galerkin approximation for magnetohydrodynamic type equations
Rodríguez-Bellido M.A., Rojas-Medar M.A. and Sepúlveda-Cerda A. **325**

Asymptotic aspects of the logistic equation under diffusion
Sabina de Lis J.C. and Segura de León S. **332**

Analysis of turbulence models for flow simulation in the aorta
Santos S., Rojas J.M., Romero P., Lozano M., Conejero J.A. and García-Fernández I. **339**

Overdetermined elliptic problems in onduloid-type domains with general nonlinearities
Wu J. **344**

XXVI Congreso de Ecuaciones Diferenciales y Aplicaciones
XVI Congreso de Matemática Aplicada
Gijón, 14-18 junio 2021
(pp. 339–343)

Analysis of turbulence models for flow simulation in the aorta

Samuel Santos[1], Jose M. Rojas[2], Pau Romero[1], Miguel Lozano[1], J. Alberto Conejero[3], Ignacio García-Fernández[1]

1. *CoMMLab, Universidad de Valencia, Burjassot, Valencia, Spain,* ignacio.garcia@uv.es
2. *Escuela Técnica Superior de Ingeniería del Diseño, Universidad Politécnica de Valencia, Valencia, Spain,* joroar1@etsid.upv.es
3. *Departmento de Matemática Aplicada, Universidad Politécnica de Valencia, Valencia, Spain,* aconejero@upv.es

Abstract

Computation of Wall Shear Stress (WSS) in the aorta wall is a relevant problem, since it has been related to the appearance of several cardiovascular diseases. In this context, our aim is to solve Navier-Stokes (NS) equations with boundary conditions in the aorta. For an accurate estimation of WSS, a proper election of the turbulence model is of great relevance. We present a study to compare WSS estimation considering three different turbulence models in the thoracic aorta and an analysis of the influence of the aortic valve. The size and properties of the appropriate mesh to use is also discussed. Our simulations are carried out with the Finite Volume Method solver OpenFoam.

1. Introduction

Computational Fluid Dynamics has become an essential tool in the study of blood flow in order to understand genesis of cardiovascular diseases. In this work we focus on the WSS reached in the toracic aorta at peak systolic conditions. Particularly, we know that low values of WSS are related to atherosclerosis, see [5]. To do so, we first need to determine what model is more appropiate to this task. On the one hand we test a model based in the NS equations and on the other hand $k-\epsilon$, $k-\omega$ and SST $k-\omega$ turbulence models which are reformulations of the first one. Once we have chosen our model we will study the influence of three types of aortic valves: a healhty valve and two prosthetic valves. This document is structured as follows: In section 2 we introduce the models of fluid likely to be chosen and the corresponding equations. In section 3 we explain tecnical details of simulations and results obtained. Finally, in section 4 we summarize, conclude and expose some improvements and future works.

2. Models and boundary conditions

Fluid dynamics is governed by NS equations, a system of coupled partial differential equations concerning fluid velocity and pressure. In this work we deal with blood flowing through aorta. In this context we can suppose that blood is an incompressible newtonian fluid. As our aim is to get WSS, we first need to compute blood flow. This requires to solve NS equations with a set of boundary conditions that, in our case, will reproduce peak systolic conditions. We also neglect time derivatives in all model considered so we are calculating instantaneous WSS in the time of maximum blood flow. We consider, in the first place, the usual stationary Navier-Stokes equations for an incompressible Newtonian fluid, given by

$$\nabla \cdot \vec{v} = 0; \qquad \vec{v} \cdot \nabla \boldsymbol{v} = -\frac{1}{\rho}\nabla p + \frac{1}{\rho}\nabla \cdot \Sigma, \tag{2.1}$$

where $\boldsymbol{v}$ is blood velocity, p is pressure, ρ is the blood density and $\Sigma = \mu\left(\nabla \boldsymbol{v} + \nabla \boldsymbol{v}^T\right)$ is the viscous stress tensor for a Newtonian fluid, with μ the viscosity of blood. We apply a zero-gradient condition in the outlet for the velocity and a non-slip condition in the aortic wall. Besides, velocity profiles in the inlet are settled trying to reproduce a healthy valve and two artificial prosthetic valves as shown in Figure 1. For pressure, we use a zero-gradient condition in the inlet and set a 0 value condition in the outlet.

The other three models are turbulence models (as $Re \sim 6500$) and are included in the context of the Reynolds-Averaged-Navier-Stokes (RANS) equations, consisting in the decomposition of each variable in a time average component and a fluctuating component. For example, $\boldsymbol{v} = \boldsymbol{V} + \boldsymbol{v}'$ where $\boldsymbol{V}$ and $\boldsymbol{v}'$ are the time averaged and the fluctuating component of velocity respectively. The average is taken in a sufficiently high time. The first RANS model considered is the $k-\epsilon$ model where turbulence is stored in the new variables

$$k = \frac{\overline{\boldsymbol{v}' \cdot \boldsymbol{v}'}}{2},$$

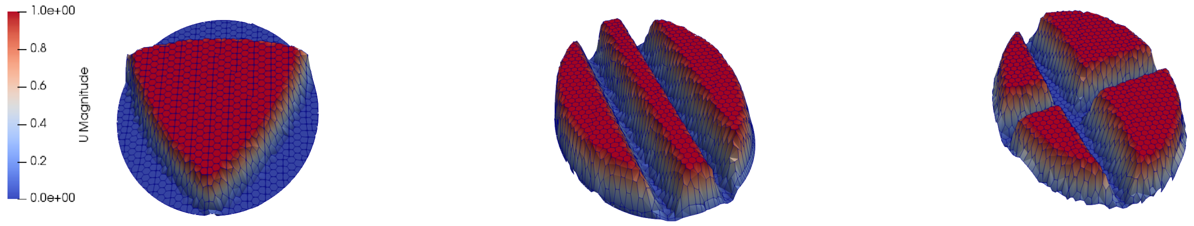

(a) Natural healthy valve. **(b)** Artificial bileaflet valve. **(c)** Artificial tilting disk valve.

Fig. 1 Vertical profile of some of the inlet boundary conditions considered. The maximum velocity is 1 m/s.

variable	inlet	wall	outlet
ϵ	2	zero gradient	zero gradient
k	10^{-6}	10^{-10}	zero gradient
ω	1	ω-wall-function	zero gradient

Tab. 1 Boundary conditions applied to turbulent variables. All units in SI.

and ϵ. k is called turbulent kinetic energy and ϵ is the rate of dissipation of k. The new equations for these variables are:

$$\boldsymbol{V} \cdot \nabla k = \frac{1}{\rho} \nabla \cdot (\mu_k \nabla k) + \frac{\mu_t}{\rho} (\Sigma' : \nabla \boldsymbol{V}) - \epsilon, \tag{2.2}$$

$$\boldsymbol{V} \cdot \nabla \epsilon = \frac{1}{\rho} \nabla \cdot (\mu_\epsilon \nabla \epsilon) + C_{\epsilon 1} \frac{\epsilon}{\rho k} (\Sigma' : \nabla \boldsymbol{V}) - C_{\epsilon 2} \frac{\epsilon^2}{k}, \tag{2.3}$$

where $\mu_t = \rho C_\mu k^2/\epsilon$ is the tubulent viscosity, $\mu_k = \mu + \mu_t/\sigma_k$ and $\mu_\epsilon = \mu + \mu_t/\sigma_\epsilon$ are effective viscosities and C_μ, $C_{\epsilon 1}$,$C_{\epsilon 2}$, σ_k and σ_ϵ are empirical constants whose values can be consulted in [6]. On the other hand

$$\Sigma' = \rho \overline{\boldsymbol{v}' \otimes \boldsymbol{v}'}$$

is the Reynolds stress tensor.

The second model used is the $k - \omega$ model. We introduce here the variable $\omega = \epsilon/(C_\mu k)$ for which an equation can be derived from (2.3). The new set of equations for the turbulent variables rest

$$\boldsymbol{V} \cdot \nabla k = \frac{1}{\rho} \nabla \cdot (\mu_k \nabla k) + \frac{\mu_t}{\rho} (\Sigma' : \nabla \boldsymbol{V}) - \beta^* k \omega, \tag{2.4}$$

$$\boldsymbol{V} \cdot \nabla \omega = \frac{1}{\rho} \nabla \cdot (\mu_\omega \nabla \omega) + C_{\alpha 1} \frac{\omega}{\rho k} (\Sigma' : \nabla \boldsymbol{V}) - C_{\beta 1} \omega^2, \tag{2.5}$$

This model has the advantage of being more precise near the wall than $k - \epsilon$ model, meanwhile the latter is more precise in the bulk flow (the stream outside the boundary layer). The last turbulence model used is the SST $k - \omega$ model which combines $k - \epsilon$ and $k - \omega$ models through blending functions. The details on the construction of this model are too extensive to be included in this document and can be consulted in [6].

Boundary conditions over the new turbulent variables are shown in table 1. We have taken considerations from [4], for k and ω where also the ω-wall-function can be read. Moreover, we have used formulas and information from [1], to settle boundary conditions on ϵ.

3. Simulation and results

We employ the Finite Volume Method solver OpenFoam to solve the previous models of NS equations in a real aorta acquired from Computerized Tomography. A mesh of about 8.6M elements with maximum spatial resolution of $50\mu m$ in the wall normal direction has been used in order to have accurate computation of the boundary layer. We will not use wall functions in the simulations presented here for pressure and velocity so we compute the entire boundary layer. A representation of the mesh used is shown in figure 2.

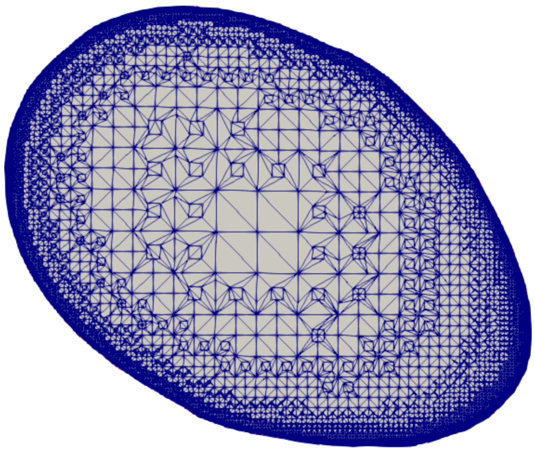

Fig. 2 Section of aorta where the mesh used was outlined.

As it can be seen a 4 refinement level is used combined with 15 extra layers in the aortic wall in order to get good WSS estimation. A Green-Gauss finite volume discretization is employed for the gradient of scalar variables. On the other hand upwind schemes are applied in divergence terms. After discretization a combination of a Gauss-Seidel method, Geometric-algebraic-multi-grid method and a smooth solver are used to solve the linear systems involved. Details can be found in [6, 7]. Also, the resolution algorithm called semi-implicit method for pressure-linked equations (SIMPLE algorithm) is employed in the conservation laws involving pressure and velocity.

Results are shown in figure 3. In the first row blood streamlines are presented, while the corresponding WSS distribution are shown below. Each column corresponds to a different model. In the first four columns a healthy valve has been settled and in the last two columns the bileaflet valve and tilting disk valve for the SST $k-\omega$ model haven been implemented.

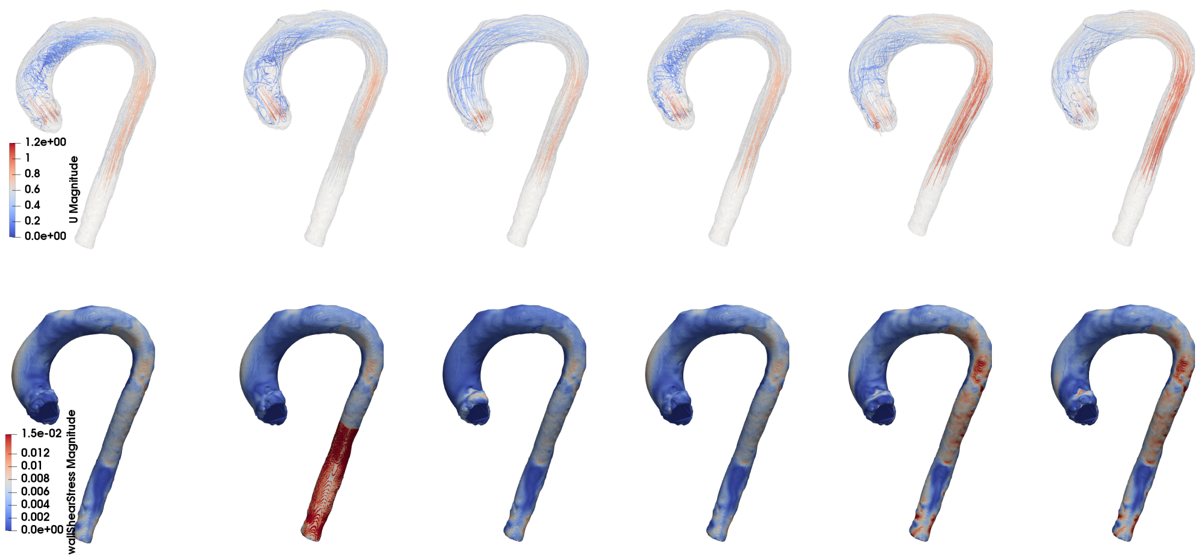

(a) No turbulence model and healthy valve.
(b) $k-\epsilon$ model and healthy valve.
(c) $k-\omega$ model and healthy valve.
(d) SST $k-\omega$ model and healthy valve.
(e) SST $k-\omega$ model and bileaflet valve.
(f) SST $k-\omega$ model and tilting disk valve.

Fig. 3 Streamlines (upper row) and WSS/ρ profiles (lower row) obtained with different turbulence models. All units in the SI.

The most remarkable result is the high values of WSS provided by the $k-\epsilon$ in the descending aorta. Since this model does not properly compute turbulence in regions with large pressure gradients (such as the boundary layer) and strong accelerations (when the aortic duct narrows), this model can be assumed to provide a poor approximation.

On the other hand, we know that the $k-\omega$ model is sensitive to boundary conditions of the turbulent variables in the inlet free stream, which does not happen with the $k-\epsilon$ model. This explains the distinct behaviour of streamlines computed with $k-\omega$ model in the cavity of the aorta. Hence, it seems that the most suitable turbulence model, out of the ones used here, is SST $k-\omega$ model. The cavity flow computed with this model looks like the one computed with $k-\epsilon$ model, which is most reliable in this region. Also, the WSS profile computed with SST $k-\omega$ model has more resemblance with the one computed with $k-\omega$ model, the one that behaves well near the wall. Not applying any turbulence model seems in good agreement with SST $k-\omega$ model. Nevertheless k is an esential parameter in the study of diseases like stenosis or coarctation. Then, SST $k-\omega$ model is the one selected from now on.

Streamlines obtained in ascending aorta with the three types of valves are trustable when comparing with experimental and theoretical works, see [2, 8]. Regarding the effect of the valve type, it clearly affects the WSS profile. We consider a WSS critical value of 0.5 Pa below which there is risk of atherosclerosis appearence. Figure 4 shows a detailed analysis of the influence of the type of valve on the WSS values. We analize 7 sections along the aorta, S_i for $1 \leq i \leq 7$. S_1, S_2 and S_3 are placed in the ascending aorta where the results are more trustworthy. We can see that in the case of the bileaflet valve almost 16% of S_1 is in risk, the highest value of the analysis, meanwhile 10% with the tilting disk valve around and 2% with the healthy valve. In S_2 there is no region in risk for any valve and in S_3 we have 6%, 5% and 4% for the healthy, bileaflet and tilting disk valve respectivelly.

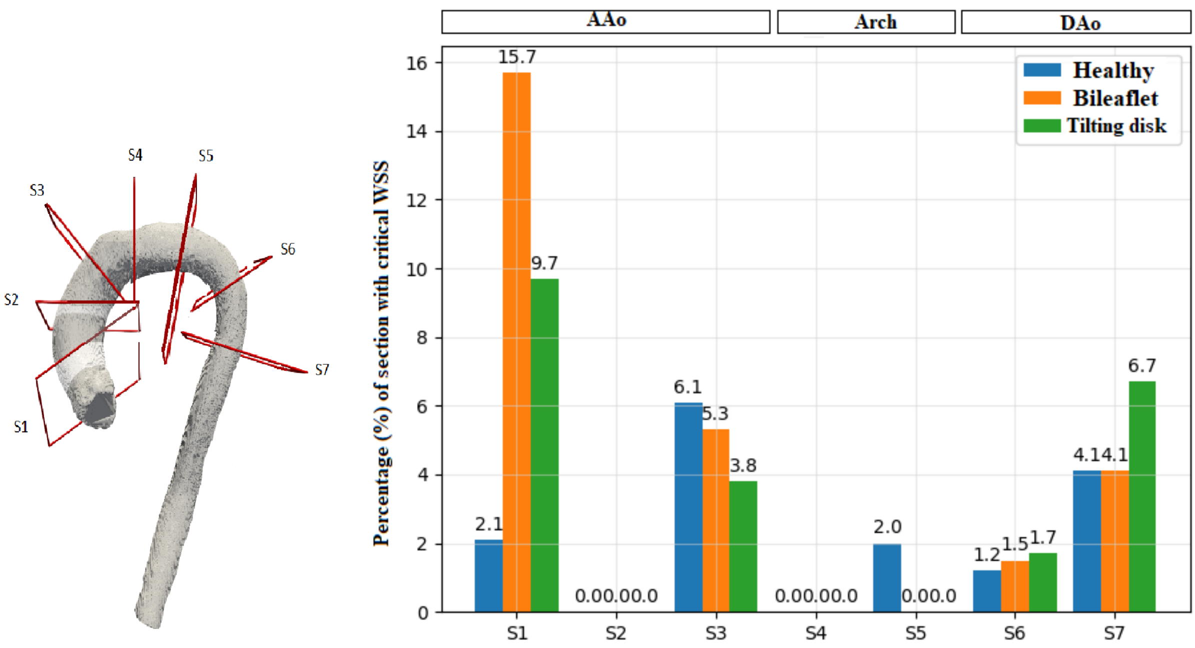

Fig. 4 Locations where sections analyzed were placed (left) and histogram of the percentage of section with critical WSS for the seven sections and for the three types of valve (right).

Values on the descending aorta are not trustable as we are neglecting the supraortic arteries which suppose the 30% of the entire flow. However, we observe an increase of the risk region with artificial valves.

4. Conclusions

First of all we made an analsys about what model of turbulence was more suitable for WSS estimation. We conclude that the SST $k-\omega$ model was the most realiable as it possesses the good properties from both $k-\epsilon$ and $k-\omega$ models and, besides, it calculates the turbulent kinetic energy k which is important in the study of cardiovascular diseases.

Concerning WSS values, it can be observed that both prosthetic valves contribute to increase them and that the bileaflet valve does it in a minor level than the tilting disk valve in the ascending aorta. Hence, we can say that the human biology has made a good work and that whenever a prosthetic valve is needed we support the bileaflet valve above the tilting disk one.

Transitory simulations to take into account the whole cardiac cycle are now taking place, so we will be able to compute other hemodynamic variables of interest as OSI or TAWSS. Also, in the future, a fluid-structure interaction should be considered to get a complete study of genesis of cardiovascular diseases.

References

[1] C. J. Greenshields. OpenFOAM user guide Version 8. The OpenFOAM Foundation, 2020.

[2] U. Gülan, B. Luthi, M. Holzner, A. Liberzon, A. Tsinober & W. Kinzelbach. Experimental study of aortic flow in the ascending aorta via particle tracking velocimetry. Experiments in fuids 53.5, pags. 1469-1485, 2012.

[3] D. A. Jones, M. Chapuis, M. Liefvendahl, D. Norrison and R. Widjaja. RANS Simulations using OpenFOAM Software. No. DST-Group-TR-3204. Defence Science and Technology Group Fishermans Bend Victoria Australia, 2016.

[4] D. Lindblad, A. Jareteg & O. Petit. Implementation and run-time mesh refinement for the $k - \omega$ SST DES turbulence model when applied to airfoils. Project work. Chalmers University of Technology, 2014.

[5] A. M. Malek, S. L. Alper & S. Izumo. Hemodynamic shear stress and its role in atherosclerosis. Jama 282.21, pags. 2035-2042, 1999.

[6] F. Moukalled, L. Mangani and M. Darwish. The finite volume method in computational fluid dynamics. Vol. 113. Berlin, Germany:: Springer, 2016.

[7] J. M. Rojas. Influencia del tipo de válvula en el flujo sanguíneo de la aorta torácica: zonas en riesgo de arterioesclerosis. Final master disertation, Escuela Técnica Superior de Ingeniería del Diseño, Universidad Politécnica de Valencia.

[8] W. Yin, Y. Alemu, K. Affeld, J. Jesty & D. Bluestein. Flowinduced platelet activation in bileaflet and monoleaflet mechanical heart valves. Annals of biomedical engineering 32.8, pags. 1058-1066, 2004.